IranJOC
Iranian Journal of
Organic Chemistry

A comparative study of glycyrrhizin and glycyrrhetinic acid complexes interactions with DNA and RNA

Shohreh Nafisi [*], Firouzeh Manouchehri and Mahyar Bonsaii

Department of Chemistry, Islamic Azad University, Central Tehran Branch (IAUCTB) Tehran, Iran, 14676 – 8683

Abstract: Spectroscopic evidence showed that glycyrrhizin and glycyrrhetinic acid bind DNA and RNA *via* major and minor grooves as well as the backbone Glycyrrhetinic acid (GA), the main metabolic product of glycyrrhizin (GL) is an aqueous extract from licorice root. These compounds are well known for their anti-inflammatory, hepatocarcinogenesis, anti-viral and interferon (IFN)-inducing activity. This study is the first attempt to investigate the binding of glycyrrhizin and glycyrrhetinic acid with DNA and RNA. The effect of the ligand complexation on DNA and RNA aggregation and condensation was investigated in aqueous solution at physiological conditions, using constant DNA and RNA concentration (6.25 mM) and various ligands /polynucleotide (phosphate) ratios of 1/240, 1/120, 1/80, 1/40, 1/20, 1/10, 1/5, 1/2 and 1/1. Fourier transform infrared (FTIR) and UV–visible spectroscopic methods were used to determine the phosphate group with overall binding constants of $K_{GL-DNA}=5.7 \times 10^3$ M^{-1}, $K_{GA-DNA}=5.1 \times 10^3$ M^{-1}, $K_{GL-RNA}=3.03 \times 10^3$ M^{-1} and $K_{GA-RNA}=2.71 \times 10^3$ M^{-1}. The affinity of ligands-DNA and -RNA binding is in the order of glycyrrhizin > glycyrrhetinic acid. DNA remains in the B-family and RNA remains in the A-family structures, while biopolymer aggregation occurred at high triterpenoid concentrations.

Keywords: DNA, Glycyrrhizin, Glycyrrhetinic acid, FTIR, UV-Visible, Docking.

Introduction

Glycyrrhetinic acid (GA) is the aglycon of glycyrrhizin (GL), a naturally occurring triterpene saponin, found as a major constituent of licorice (the root of *Glycyrrhiza* spp.). Licorice extracts contain many components, including glycyrrhizin, various sugars, flavonoids, and saponoids. GA and its related compounds are known to possess anti-inflammatory activity, and GL has been clinically used in the treatment of hepatic inflammation.

Glycyrrhizin, accounting for 10 – 25 % of licorice root extract, is considered the primary ingredient [1]. Glycyrrhizin (3-O-(2-O-β-D-Glucopyranuronosyl-α-D-glucopyranuronosyl)-18β-glycyrrhetinic acid) (GL): is hydrolyzed to 18β-glycyrrhetinic acid (3β-Hydroxy-11-oxo-18β, 20β-olean-12-en-29-oic acid (GA), (Figure **1**) in vivo, which is responsible for most of its pharmacological properties.

*Corresponding author. Tel: (+98) 21 22424565, Fax: (+98) 21 22424565, E-mail: drsnafisi@yahoo.com

Figure 1: Chemical structure of glycyrrhizin (GL) and 18β-glycyrrhetinic acid (GA)

It has been used in clinic as a remedy for the treatment of chronic hepatitis [2], tumorigenic [3,4] and human immunodeficiency virus (HIV) infection [5,6]. Special attention is attracted by the ability of GL to suppress reproduction of some DNA and RNA viruses, including the human immunodeficiency virus,

inactivating herpes simplex virus particles irreversibly [7,8]. Glycyrrhizin inhibits liver cell injury caused by many chemicals and is used in the treatment of chronic hepatitis and cirrhosis in Japan. Presumably, GL inhibits the protein kinase activity [7,8]. Several proteins have been reported to serve as GL targets. These are mostly casein kinase II (CK-II) substrates such as lactoferrin or lipoxigenase [9,10]. Recombinant HIV-1 reverse transcriptase has been shown to efficiently bind with recombinant human CK-II and to require phosphorylation for its normal enzymic activity [11]. Acting as a CK-II inhibitor, GL used at a high (100 mM) concentration completely inhibits phosphorylation of reverse transcriptase, which may account for its antiviral activity [7].

Glycyrrhetinic acid is a pentacyclic triterpenoid derivative of the β-amyrin. GA is effective against chronic hepatitis but is also related to the side-effect aldosteronism. Since only glycyrrhetinic acid appears in the blood circulation after oral administration, it is considered to play an important role in the biological action of oral administration [12,13].

The understanding of the mechanism of GA action may expedite development of new drugs based on GA or its derivatives and reduce the risk of side effects. This study was of our interest to examine the interaction of DNA and RNA adducts with two pentacyclic triterpenoid derivatives GL and GA in aqueous solution at pH 6-7 with ligands /DNA and RNA (P) molar ratios of 1/240 to 1/1 using FTIR and 0.005-0.1 mM by UV measurements as well as molecular modeling. Structural analyses regarding the glycyrrhizin (GL) and glycyrrhetinic acid (GA) binding sites, binding constants, DNA and RNA secondary structure are provided. Our spectroscopic results provide a major structural analysis of triterpenoids–biopolymers interaction, which helps elucidate the nature of this biologically important complexation *in vitro*.

Results and discussion

FTIR spectra of glycyrrhizin–DNA and glycyrrhetinic acid –DNA adducts

The IR spectral features of glycyrrhizin and glycyrrhetinic acid –DNA interaction are presented in Figure **2**. The plots of the relative intensity (R) of several peaks of DNA, glycyrrhizin and glycyrrhetinic acid–DNA complexes in-plane vibrations are shown in Figure **3**.

Figure 2: FTIR spectra in the region of 1800-600 cm^{-1} for calf thymus DNA, and (A) glycyrrhizin (GL), (B)

glycyrrhetinic acid (GA) adducts in aqueous solution at pH=7. DNA and two complexes spectra obtained at various GL, GA-DNA (phosphate) molar ratios (top three spectra), ligand and two difference spectra (bottom three spectra).
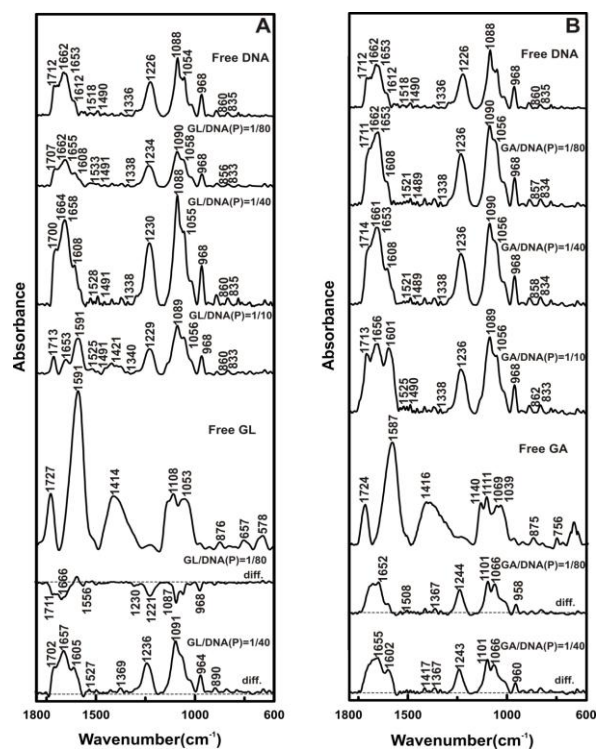
At r=1/240, no major GL–DNA interaction was observed as a result of minor spectral changes (intensity and shifting) of the guanine at 1712, thymine at 1662, adenine at 1612, cytosine at 1490 and the PO$_2$ band at 1226 cm^{-1} (asymmetric stretch) [14-19]. At higher concentrations (r=1/120), the guanine band at 1712 shifted to 1706 cm^{-1}, the thymine band at 1662 shifted to 1663 cm^{-1}, the adenine band at 1612 shifted to 1608 cm^{-1} and phosphate asymmetric band at 1226 shifted to 1234 cm^{-1}. The shifting was accompanied by intensity increase for the mainly guanine and thymine bands. The observed spectral changes can be related to glycyrrhizin interaction with bases; guanine, adenine N7, thymine O2 and backbone phosphate group.

At r= 1/80, decrease in the intensity of bases bands can be related to DNA stabilization upon glycyrrhizin interaction. At a higher glycyrrhizin concentration (r=1/40), the guanine band at 1712 shifted to 1700 cm^{-1}, the thymine band at 1662 shifted to 1664 cm^{-1}, the adenine band at 1612 shifted to 1608 cm^{-1} and phosphate asymmetric band at 1226 shifted to 1230 cm^{-1}.

Major intensity increase was observed for the guanine, thymine, adenine and phosphate at this concentration (Figures **2**A, **3**A). The observed spectral

changes are due to the major interaction of glycyrrhizin with bases and phosphate at this concentration. In the difference spectrum of glycyrrhizin-DNA (r= 1/40), the positive features at 1702, 1657, 1605, 1236 and 1091 cm^{-1} are due to an increase in intensity of the DNA vibrations as a result of glycyrrhizin interaction with the G and A-T base pair and phosphate backbone group (Figure **2**A, diff. **3**A).
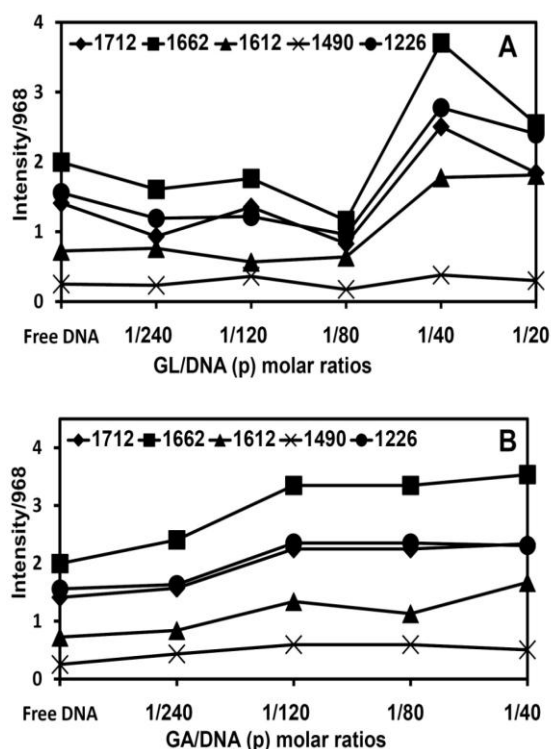

Figure 3: Intensity ratio variations for several DNA in-plane vibrations as a function of GA and GL concentration. (A) Intensity ratios for the DNA bands at 1712 (G, T), 1662 (T, G, A, C), 1612 (A), 1490 (C,G) and 1226 (PO2 asymmetric) referenced to the DNA band at 968 cm^{-1}.

At r=1/20, a major decrease in intensity was observed for the bases and phosphate vibrations which is attributed to DNA aggregation in the presence of high glycyrrhizin concentrations (Figure **3**A).

It should be noted that glycyrrhizin-PO$_2$ binding occurred at all concentrations. Evidence for this comes from major shifting of the PO$_2$ asymmetric vibration from 1226 to 1230-1234 cm^{-1} (r=1/240 to 1/20) (Figure **3**A). The observed shifting was accompanied by the variations in the intensity of the phosphate band at all concentrations (r=1/240 to 1/40). The major intensity increase at r=1/40 is related to the maximum GL-phosphate interaction at this concentration.

In addition to a major spectral shifting of the PO$_2$ asymmetric band, the relative intensities of the

asymmetric (v_{as}) and symmetric (v_s) vibrations were altered upon phosphate interaction [20]. The v_s PO$_2$ (1088 cm^{-1}) and v_{as} PO$_2$ (1226 cm^{-1}) were changed, with the ratio v_s/v_{as} going from 1.7 (free DNA) to 1.9 (glycyrrhizin-DNA complexes) at a high glycyrrhizin concentration (Figure **2**A). This showed that the maximum binding of glycyrrhizin to backbone phosphate group occurs at r=1/40.

No major intensity changes were observed for the cytosine band at 1490 cm^{-1} that is indicative of no major participation of cytosine in glycyrrhizin–DNA binding.

It is worth mentioning that the absorption bands with medium intensity at 1653 cm^{-1} in the IR spectrum of free DNA and at 1651–1654 cm^{-1} in spectra of the glycyrrhizin–DNA adducts and in difference spectra are due to water deformation mode, and they are not coming from DNA vibrations [21].

At low glycyrrhetinic acid concentration (r=1/240, 1/120), major interaction was observed as a result of spectral changes in the glycyrrhetinic acid-DNA interaction at this concentration. The guanine band at 1712 shifted to 1714 cm^{-1} (r=1/240, 1/120), the thymine band at 1662 shifted to 1666 cm^{-1} (r=1/240, 1/120), the adenine band at 1612 shifted to 1606 cm^{-1} (r=1/240), 1608 (r=1/120) and the phosphate asymmetric band at 1226 shifted to 1236 cm^{-1} (r=1/240, 1/120). The observed shifting was accompanied by intensity increase of the guanine, adenine and mainly thymine and phosphate bands upon glycyrrhetinic acid complexation. A gradual increase of intensity of DNA vibrations with a maximum at r=1/120 indicating a major interaction of glycyrrhetinic acid with DNA bases at this concentration No major intensity change was observed at r=1/80, 1/40 indicating no more interaction at higher concentrations (Figures **2**B and **3**B).

Additional evidence regarding glycyrrhetinic acid interaction with phosphate backbone group comes from the relative intensities of the asymmetric (v_{as}) and symmetric (v_s) vibrations of the phosphate group [20]. The v_s PO$_2$ (1088 cm^{-1}) and v_{as} PO$_2$ (1226 cm^{-1}) were changed, with the ratio v_s/v_{as} going from 1.7 (free DNA) to 1.5 (glycyrrhetinic -DNA complexes) upon glycyrrhetinic acid complexation (Figure **2**B).

Absorption spectroscopy revealed that addition of the aqueous glycyrrhizin and glycyrrhetinic acid to DNA solution resulted a red shift of the DNA band at 258 to 260–263 nm in complexes, which is additional evidence for glycyrrhizin and glycyrrhetinic acid - DNA interaction (Figures **4**A, **4**B).
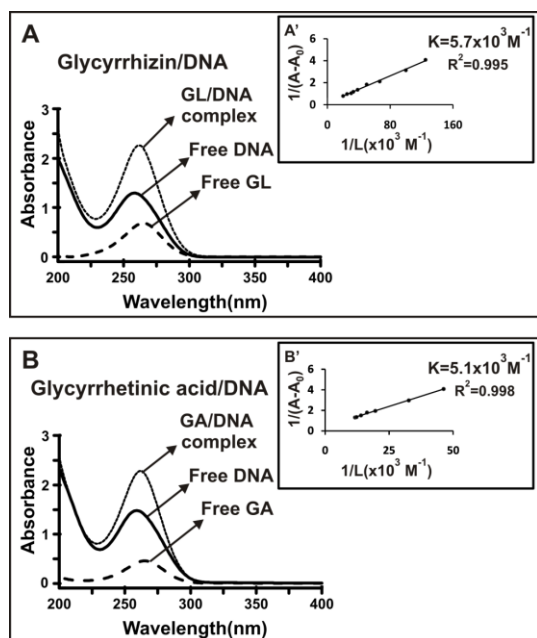
Figure 4: UV-visible results of calf-thymus DNA and (A) glycyrrhizin (GL), (B) glycyrrhetinic acid (GA) complexes: spectra of free DNA (0.5 mM); free GL, GL–DNA complex (0.03 mM); free GA, GA–DNA complex (0.08mM). Plot of $1/(A–A_0)$ versus (1/ligand concentration) for GL, GA and calf-thymus DNA complexes, where A_0 is the initial absorbance of DNA (258 nm) and A is the recorded absorbance at different GL, GA concentrations (0.005–0.1 mM) with constant DNA concentration of 0.5 mM at pH 7.

Infrared spectra of glycyrrhizin and glycyrrhetinic acid –RNA adducts

The spectral changes (intensity and shifting) of several prominent RNA in-plane vibrations at 1698 (G, U, mainly G), 1651 (U, G, A, and C, mainly U), 1609 (A, C, mainly A), 1491 (C, G, mainly C), and 1241 cm^{-1} (PO$_2$ asymmetric stretch) [16,18,22-27] were monitored at different glycyrrhizin and glycyrrhetinic acid–RNA molar ratios, and the results are shown in Figure **5**. The plots of the relative intensity (R) of several peaks of RNA, glycyrrhizin and glycyrrhetinic acid–RNA complexes in-plane vibrations are shown in Figure **6**. *The intensities of the bands (Free GL and GA, GL and GA/RNA=1/2, diff. GL and GA/RNA=1/2) are halved.

In the glycyrrhizin-RNA complexes, major interaction was observed with mainly guanine, and uracil bases, and to a lesser extent with adenine and backbone phosphate group. Evidence for this comes from spectral changes (intensity and shifting) of the

bases and PO$_2$ bands upon glycyrrhizin complexation (Figures **5**A, **6**A).
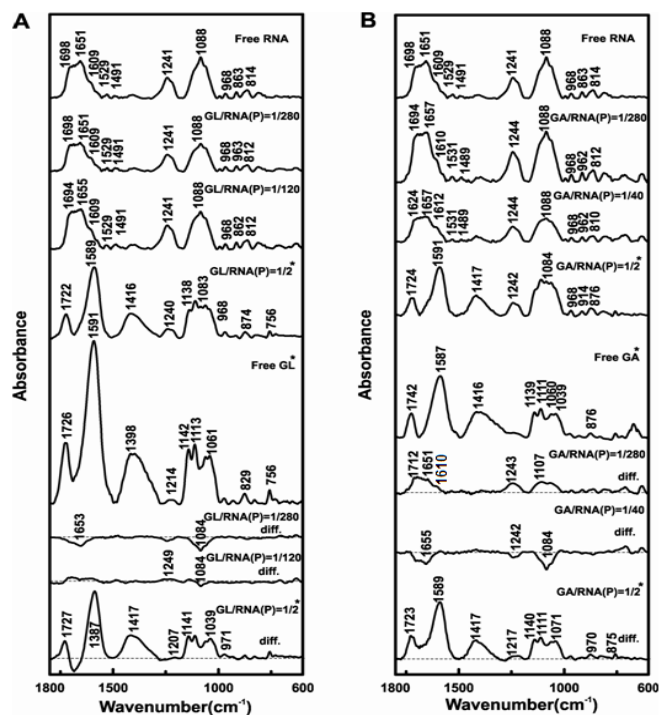
Figure 5: FTIR spectra and difference spectra [(RNA solution + ligand solution) -(RNA solution)] in the region of 1800-600 cm-1 for yeast RNA (6.25 mM), and (A) Glycyrrhizin-RNA; (B) Glycyrrhetinic acid-RNA (0.1–12.5 mM) adducts in aqueous solution at pH=7. RNA and three complexes spectra obtained at various GL, GA-RNA (phosphate) molar ratios (top four spectra), ligand and three difference spectra (bottom four spectra).

At r=1/280, 1/240, intensity of the guanine band at 1698 cm^{-1}, uracil band at 1651 cm^{-1}, and the adenine band at 1609 cm^{-1} decreased as s result of RNA aggregation in the presence of glycyrrhizin (Figures **5**A, **6**A). No major shifting was observed at r=1/280, however at r=1/240 to 1/40, the guanine band at 1698 shifted to 1694-1693 cm^{-1} and the uracil band at 1651 shifted to 1658-1657 cm^{-1}. The observed shifting can be related to major interaction of glycyrrhizin with guanine N7 and uracil O2 (Figure **5**A). At r=1/120, the intensity of the guanine band at 1698 cm^{-1}, the uracil band at 1651 cm^{-1} and the adenine band at 1609 cm^{-1} increased (Figures **5**A, **6**A) that can be related to major interaction of glycyrrhizin with guanine, uracil and to a lesser extent with adenine bases. At r= 1/80, the intensity of the bases decreased as a result of RNA aggregation upon glycyrrhizin-RNA complexation (Figure **6**A). At r=1/40, the intensity of the guanine, uracil and adenine bands augmented as a result of

RNA destabilization upon glycyrrhizin interaction with guanine and adenine (N7) and uracil (O2) (Figure **6**A). At higher GL concentrations (r=1/20 to 1/1), monitoring the spectral changes of the RNA bands was not possible, because the RNA bases vibrations overlapped with glycyrrhizin absorption bands at 1726 and 1591 cm^{-1} (Figure **5**A ; r=1/2 is shown here). It is worth mentioning that minor spectral changes were observed for the cytosine band at 1491 cm^{-1} upon glycyrrhizin interaction, which is indicative of minor participation of cytosine bases in glycyrrhizin complexation (Figure **6**A).
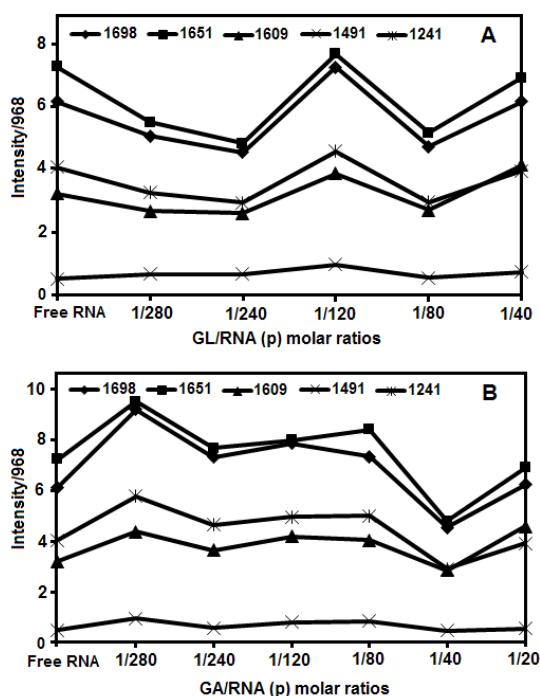
Figure 6: Intensity ratio variations for several RNA in-plane vibrations as a function of (A) GL and (B) GA concentrations (0.1–12.5 mM). Intensity ratios for the RNA bands at 1698 (G), 1651 (U), 1609 (A), 1491 (C) and 1241 (PO2) cm^{-1} referenced to the RNA band at 968 cm^{-1}.

For the backbone PO$_2$ asymmetric stretching, no major shifting was observed for the phosphate band at 1241 cm^{-1} upon glycyrrhizin complexation (r=1/240 to 1/40) (Figure **5**A). However, decrease and increase in intensity of the PO$_2$ band can be related to glycyrrhizin interaction with backbone phosphate group (Figure **6**A).

In the difference spectra of glycyrrhizin-RNA (r=1/280, 1/80) (Figure **5**A, r=1/80 is not shown here), the reduction in intensity is related to major RNA aggregation in the presence of glycyrrhizin. In the difference spectra of glycyrrhizin-RNA (r= 1/20 to

1/1), the positive features at 1731-1722 cm^{-1}, 1589-1587 cm^{-1}, 1419-1413 cm^{-1} are coming from glycyrrhizin vibrations not from RNA vibrations (Figure **5**A, diff r= 1/2 is shown here).

Evidence related to glycyrrhetinic acid–RNA complexation comes from the infrared spectroscopic results shown in Figures **5**B and **6**B. In the glycyrrhetinic acid–RNA complexes, GA binds mainly to guanine and uracil bases and to a lesser extent to adenine and the backbone PO$_2$ group (Figure **6**B). Evidence for this comes from spectral changes of the bases and phosphate bands upon GA interaction (Figures **5**B, **6**B).

At lower concentrations (r=1/280), no major shifting was observed for the bases and phosphate bands, however at r= 1/240 to 1/20, the guanine band at 1698 cm^{-1} shifted toward a lower frequency at 1694-1692 cm^{-1}, the uracil band at 1651 shifted to 1657 cm^{-1}. For the adenine band at 1609 cm^{-1}, no major shifting was observed at lower concentrations (r=1/280, 1/240), however at higher concentrations (r=1/40, 1/20), it shifted to a higher frequency at 1612 cm^{-1} (Figure **5**B; r= 1/20 is not shown here). At r=1/280, the intensity of the guanine, uracil and to a lesser extent, adenine and phosphate bands increased as a result of major interaction of glycyrrhetinic acid with guanine, uracil, adenine bases and backbone phosphate group. At r=1/240, the intensity of the bases and phosphate bands decreased which can be related to RNA aggregation upon GA interaction. No major interaction was observed for the adenine, guanine and phosphate bands at higher concentrations (r=1/120, 1/80) due to minor intensity changes of the bands upon GA interaction. At r=1/40, the intensity of the bases and phosphate bands decreased that can be related to RNA aggregation upon GA interaction (Figure **6**B).

No major spectral changes was observed for the cytosine band at 1491 cm^{-1} (r=1/280 to 1/20), that can be related to no major participation of cytosine in GA–RNA bindings.

In the difference spectra of glycyrrhetinic acid-RNA (r=1/280), the positive features at 1712, 1651, 1610 and 1243, 1107 cm^{-1} (Figure **5**B, Diff. r=1/280) are due to the intensity increase of the guanine, uracil, adenine and phosphate bands upon glycyrrhetinic acid complexation and approves major interaction of glycyrrhetinic acid with guanine and adenine N7, uracil O2 and backbone PO$_2$ group.

Additional evidence regarding glycyrrhizin and glycyrrhetinic acid-RNA interaction comes from UV results that showed an increase in intensity of the RNA band at 258 nm due to the interaction of glycyrrhizin

with RNA strand (Figures **7**A, **7**B). Similar spectral changes were observed in the flavonoids–RNA complexes [28].
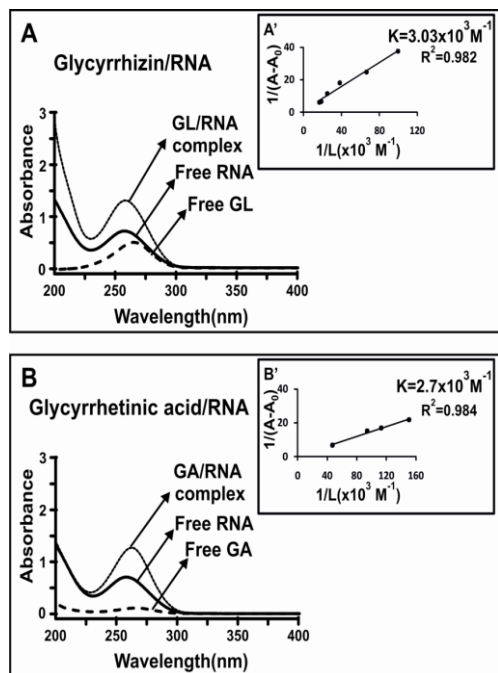

Figure 7: UV-visible results of RNA and (A) glycyrrhizin (GL), (B) glycyrrhetinic acid (GA) complexes; spectra of free RNA (0.5 mM); free GL, GL–RNA complex (0.03 mM); free GA, GA–RNA complex (0.06 mM). Plot of $1/(A–A_0)$ versus (1/ ligand concentration) for GL, GA and RNA complexes, where A_0 is the initial absorbance of RNA (258 nm) and A is the recorded absorbance at different GL, GA concentrations (0.005–0.1 mM) with constant RNA concentration of 0.5 mM at pH 7.

DNA and RNA conformations

No alterations of B–DNA structure were observed upon glycyrrhizin and glycyrrhetinic acid-DNA complexation as a result of no major spectral changes for B–DNA marker bands at 1226 cm^{-1} (PO$_2$ stretch), 1712 cm^{-1} (mainly guanine) and 836 cm^{-1} (phosphodiester mode) upon glycyrrhizin and glycyrrhetinic acid complexation [16,18,21] (Figures **2**,**5**).

In a B to A transition, the marker band at 836 cm^{-1} shifts towards a lower frequency at about 825-800 cm^{-1} and the guanine band at 1712 cm^{-1} appears at 1700-1695 cm^{-1}, while the phosphate band at 1226 cm^{-1} shifts towards a higher frequency at 1240-1235 cm^{-1} [21,29]. In a B to Z conformational changes, the sugar–phosphate band at 836 cm^{-1} appears at 800–780 cm^{-1}, and the guanine band displaces to 1690 cm^{-1}, while the phosphate band shift to 1216 cm^{-1} [21,29]. In the glycyrrhizin and glycyrrhetinic acid-DNA complexes, shifting of the B-DNA marker bands at 1226 to 1230–1238 cm^{-1} is indicative of GL and GA interaction with phosphate and not arising from B to A-DNA conformational change [30-32] (Figures **2**A, **2**B).

RNA also remains in A-conformation in glycyrrhizin and glycyrrhetinic acid–RNA complexes. Evidence for this comes from presence of the marker infrared bands at 1698 (G), 1241 (PO$_2$), 863 (ribosephosphate) and 814 cm^{-1} (phosphodiester mode), which are due to RNA in A-conformation [31-34]. In the glycyrrhizin and glycyrrhetinic acid–RNA complexes, the lack of major shifting of RNA marker bands at 1700–1688 (guanine), 1247–1241 (phosphate), 867–861 (ribose-phosphate), and 815–809 cm^{-1} (phosphodiester) is indicative of RNA remaining in A-conformation upon GL and GA complexation (Figures **5**A, **5**B). In the glycyrrhizin and glycyrrhetinic acid–RNA complexes, the shifting of the guanine band at 1698 to 1694 cm^{-1} can be related to GL and GA interaction with guanine and it is not coming from RNA conformational change.

Stability of glycyrrhizin, glycyrrhetinic acid -DNA and RNA complexes

The ligand binding constants were determined as described in Materials and Methods (UV–visible spectroscopy). The calculations of the overall binding constants were carried out using UV spectroscopy as reported [35]. Concentrations of the complexed ligand were determined by subtracting absorbance of the free DNA and RNA at 258 nm from those of the complexed. Concentration of the free ligand was determined by subtraction of the complex ligand from total ligand used in the experiment. Our data of 1/[ligand complex] almost proportionally increased as a function of 1/[free ligand] (Figures **4**,**7**). The double reciprocal plot of $1/(A-A_0)$ versus 1/(ligand concentration) is linear, and the binding constant (K) can be estimated from the ratio of the intercept to the slope (Figuers **4**,7), where A_0 is the initial absorbance of the free DNA and RNA at 258 nm, and A is the recorded absorbance of DNA and RNA in the presence of different glycyrrhizin and glycyrrhetinic acid concentrations. The overall binding constant is estimated to be $K_{GL-DNA}= 5.7 \times 10^3$ M^{-1}, $K_{GA-DNA}= 5.1 \times 10^3$ M^{-1}, $K_{glycyrrhizin-RNA}= 3.03 \times 10^3$ M^{-1} and $K_{glycyrrhetinic\ acid-RNA}= 2.71 \times 10^3$ M^{-1}. The binding constants of glycyrrhizin and glycyrrhetinic acid-DNA and -RNA binding is in the order of glycyrrhizin > glycyrrhetinic acid. Similar binding constants were estimated for alkaloids and taxol-RNA complexes [28,36].

Conclusion

Based on our spectroscopic results, the following points are important;

Glycyrrhizin and glycyrrhetinic acid interact with DNA and RNA *via* external binding. In GL and GA-DNA complexes, glycyrrhizin binding is via G, A, T and PO_2, while glycyrrhetinic acid interacts with A, T and PO_2 backbone group of DNA.

In GL and GA-RNA complexes, GL and GA interact with RNA bases via guanine, adenine N7, uracil O2, and backbone phosphate group (PO_2).

The affinity of GL-DNA, -RNA and GA-DNA, -RNA is in the order of GL-DNA > GA-DNA > GL-RNA > GA-RNA. GL and GA binding to DNA is stronger, since DNA is double helix, but RNA is not. GL-DNA, -RNA complexes are more stable than GA-DNA, -RNA complexes. The presence of extra oxygen atoms in glycyrrhizin can have more hydrated water molecules and thus extra H-bonding with DNA and RNA bases, which leads to extra stability for glycyrrhizin over glycyrrhetinic acid. No DNA and RNA conformational changes were observed upon GL and GA complexation, while biopolymer aggregation occurred at higher GL and GA concentrations.

The affinity of ligands –DNA and RNA binding is in the order of glycyrrhizin > glycyrrhetinic acid. Higher stability was observed for GL and GA-DNA complexes rather than GL and GA-RNA adducts.

Experimental

Materials and Methods

Materials

DNA sodium salt, yeast Baker RNA sodium salt, glycyrrhizin and glycyrrhetinic acid were purchased from Sigma Chemical (St. Louis, MO) and used without further purification. To check the protein content of DNA solutions, the absorbance bands at 258 and 280 nm were used. The A258/A280 ratio was 2.10 for DNA and RNA, showing that DNA samples were sufficiently free from protein [37]. Other chemicals were of reagent grade and used without further purification.

Preparation of stock solutions

DNA and RNA was dissolved to 0.5% w/v (0.0125 M) polynucleotide (phosphate) (pH 7) in NaCl solution for 24 h with occasional stirring to ensure the formation of a homogeneous solution. The final concentration of the DNA and RNA solutions were determined spectrophotometrically at 258 nm using molar extinction coefficient $\varepsilon_{258}= 9250$ cm^{-1} M^{-1} (DNA and RNA) (expressed as molarity of phosphate groups) [38].

The appropriate amount of glycyrrhizin and glycyrrhetinic acid (0.05–12.5 mM) were dissolved in water and added dropwise to DNA and RNA solutions (12.5 mM) to attain the desired ligand /DNA (P) molar ratios (r) of 1/240, 1/120, 1/80, 1/40, 1/20, 1/10, 1/5, 1/2 and 1/1 and ligand/ RNA molar ratios (r) of 1/280, 1/240, 1/120, 1/80, 1/40 and 1/20 with a final DNA(P) and RNA concentrations of 6.25 mM. The pH values of solutions were adjusted at 7.0±0.2 using by NaCl solution. The infrared spectra were recorded 2 h after mixing of the GL and GA with DNA and RNA solutions. For UV measurements, the ligand concentrations of 0.005 – 0.1 mM were used with constant DNA and RNA concentrations of 0.5 mM.

FTIR spectroscopy measurements

Infrared spectra were recorded on a Nicolet FTIR spectrometer (Magna 550) equipped with a liquid-nitrogen-cooled HgCdTe(MCT) detector and a KBr beam splitter. The spectra of ligands /DNA and RNA solutions were taken using a cell assembled with ZnSe windows. Spectra were collected and treated using the OMNIC software supplied by the manufacturer of the spectrophotometer. The spectra of the solutions were recorded after 2 h incubation of ligands with DNA and RNA solutions, using ZnSe windows. The bands were measured in triplicates (three individual samples of the same DNA and RNA and ligand concentrations). For each spectrum, 100 scans were collected with resolution of 4 cm^{-1}. The difference spectra [(polynucleotide solution + ligand solution) - (polynucleotide solution)] were obtained using a sharp DNA and RNA band at 968 cm^{-1} as internal reference [39,40]. This band, which is due to sugar C-C and C-O stretching vibrations, exhibits no spectral change (shifting or intensity variation) upon ligand –DNA and –RNA complexation, and cancelled out upon spectral subtraction.

The intensity ratios of the bands due to several DNA and RNA in plane vibrations related to A-T (for DNA) and A-U (for RNA), G-C base pairs and the PO_2 stretching vibrations were measured with respect to the reference bands at 968 cm^{-1} (DNA and RNA) as a function of ligand concentrations with an error of ±3%. Similar intensity variations have been used to determine the ligand binding to DNA and RNA bases and backbone phosphate groups [41].

The plot of the relative intensity (R) of several peaks of DNA in-plane vibrations related to A-T, G-C base pairs and the PO_2 stretching vibrations such as 1712 (guanine), 1662 (thymine), 1612 (adenine), 1490 (cytosine), and 1226 cm^{-1} (PO_2 groups), and the plot of the relative intensity (R) of several peaks of RNA in-plane vibrations related to A-U, G-C base pairs and the PO_2 stretching vibrations such as 1698 (guanine), 1651(uracil), 1609 (adenine), 1491 (cytosine), and 1241 cm^{-1} (PO_2 groups), versus ligand concentrations were obtained after peak normalization using $R_i = I_i/I_{968}$, where I_i is the intensity of the absorption peak for pure DNA and RNA in the complex with i as the ligand concentration, and I_{968} is the intensity of the 968 cm^{-1} peak (DNA and RNA internal reference).

The plots of intensity were drawn from r=1/240 to 1/20 for glycyrrhizin-DNA; r=1/240 to 1/40 for glycyrrhetinic acid-DNA; r=1/280 to 1/40 for GL-RNA and to 1/20 for GA-RNA.

At higher GL and GA concentrations (for GL- and GA-DNA, r=1/40 and to 1/1 and for GL-RNA; r=1/40 to 1/1 and for GA-RNA; r=1/20 to 1/1), due to the overlapping of the glycyrrhizin and glycyrrhetinic acid absorption bands with DNA and RNA vibrations, monitoring the intensity changes of DNA and bands were not possible.

Absorption spectroscopy

The absorption spectra were recorded on a LKB model 4054 UV–visible spectrometer, quartz cuvettes of 1 cm were used and the absorption spectra recorded with ligand concentrations of 0.005 – 0.1mM and constant polynucleotide concentration of 0.5mM. The binding constants of the ligand-DNA complexes were calculated as reported [35]. It is assumed that the interaction between the ligand [L] and the substrate [S] is 1:1; for this reason a single complex SL (1:1) is formed.

The relationship between the observed absorbance change per centimeter and the system variables and parameters is as follow;

$$\frac{\Delta A}{b} = \frac{S_t K_{11} \Delta \varepsilon_{11} [L]}{1 + K_{11}[L]} \qquad (1)$$

Where $\Delta A = A - A_o$ from the mass balance expression $S_t = (S) + (SL)$, we get $(S) = S_t/(1 + K_{11}(L))$.

Equation (1) is the binding isotherm, which shows the hyperbolic dependence on free ligand concentration. The double-reciprocal form of plotting the rectangular hyperbola $\frac{1}{y} = \frac{f}{d} \cdot \frac{1}{x} + \frac{e}{d}$, is based on the linearization of equation (1) according to the following equation,

$$\frac{b}{\Delta A} = \frac{1}{S_t K_{11} \Delta \varepsilon_{11}[L]} + \frac{1}{S_t \Delta \varepsilon_{11}} \qquad (2)$$

Thus the double reciprocal plot of $1/\Delta A$ versus $1/(L)$ is linear and the binding constant can be estimated from the following equation

$$K_{11} = \frac{intercept}{slope} \qquad (3)$$

References

[1] Eisenbrand, G. *Mol. Nutr. Food Res.* **2006**, *50*, 1087.

[2] Van Rossum, T. G.; Vulto, A. G.; de Man, R. A.; Brouwer, J. T.; Schalm, S. W. Aliment. *Pharmacol. Ther.* **1998**, *12*, 199.

[3] Lee, C. S.; Kim, Y.J.; Lee, M. S.; Han, E. S.; Lee, S. *J. Life Sci.* **2008**, *83*, 481.

[4] Nishino, H.; Kitagawa, K.; Iwashima, A. *Carcinogenesis* **1984**, *5*, 1529.

[5] Hattori, T.; Ikematsu, S.; Koito, A.; Matsushita, S.; Maeda, Y. *Antivir. Res.* **1989**, *11*, 255.

[6] Salvi, M.; Fiore, C.; Armanini, D.; Toninello, A. *Biochemical pharmacology* **2003**, *66*, 2375.

[7] Harada, S.; Haneda, E.; Maekawa, T.; Morikawa, Y.; Funayama, S.; Nagata, N.; Ohtsuki, K. *Biol. Pharm. Bull.* **1999**, *22*, 1122.

[8] Pompei, R.; Flore, O.; Marccialis, M. A.; Pani, A.; Loddo, B. *Nature* **1979**, *281*, 689.

[9] Hatomi, M.; Tanigawa, K.; Fujihara, M.; Ito, J.; Yanahira, S. *Biol. Pharm. Bull.* **2000**, *23*, 1167.

[10] Shimoyama, Y.; Ohtaka, H.; Nagata, N.; Munakata, H.; Hayashi, N.; Ohtsuki, K. *FEBS Lett.* **1996**, *391*, 238.

[11] Harada, S.; Maekawa, T.; Haneda, E.; Morikawa, Y.; Nagata, N. *Biol. Pharm. Bull.* **1998**, *21*, 1282.

[12] Ishida, S.; Sakiya, Y.; Ichikawa, T.; Awazu, S. *Chem. Pharm. Bull.* **1989**, *37*, 2509.

[13] Oketani, Y.; Takehara, I.; Mikuni, H.; Shiraishi, T.; Wakamatsu, K.; Watanabe, H.; Tanaka, T. *Clin. Rep.* **1985**, *19*, 197.

[14] Marmur, J.; Doty, P. *J. Mol. Biol.* **1961**, *3*, 585.

[15] Vijalakshmi, R.; Kanthimathi, M.; Subramania, V. *Biochem. Biophys. Res. Commun.* **20002**, *71*, 731.

[16] Kanakis, C. D.; Tarantilis, P. A.; Polissiou, M. G.; Diamantoglou, S.; Tajmir-Riahi, H. A. *J. Biomol. Struct. Dyn.* **2005**, *22*, 719.

[17] Kanakis, C. D.; Tarantilis, P. A.; Polissiou, M. G.; Diamantoglou, S.; Tajmir-Riahi, H. A. *Cell biochem. Biophys.* **2007**, *49*, 29.

[18] Arakawa, H.; Ahmad, R.; Naoui, M.; Tajmir-Riahi, H. A. *J. Biol. Chem.* **2000**, *275*, 10150.

[19] Connors, K. A.: *Binding constants: the measurement of molecular complex stability*; Wiley: New York, 1987.

[20] Andrushchenko, V.; Leonenko, Z.; Cramb, D.; van de Sande, H.; Wieser, H. *Biopolymers* **2001**, *61*, 243.

[21] Dovbeshko, G. I.; Chegel, V. I.; Gridina, N. Y.; Repnytska, O. P.; Shirshov, Y. M.; Tryndiak, V. P. *Biopolymers* **2002**, *67*, 470.

[22] Loprete, M.; Hartman, K.A. *Biochemistry* **1993**, *32*, 4077.

[23] Ahmed Ouameur, A.; Tajmir-Riahi, H. A. *J. Biol. Chem.* **2004**, *279*, 42041.

[24] Taillandier, E.; Liquier, *J. Methods enzymol.* **1992**, *211*, 307.

[25] Theophanides, T.; Tajmir-Riahi, H. A. *J. Biomol. Struct. Dyn.* **1985**, *2*, 995.

[26] Dupuis, A.S. *Inorg. Chim. Acta* **1989**, *157*, 271.

[27] Tajmir-Riahi, H. A.; Neault, J. F.; Naoui, M. *FEBS Lett.* **1995**, *370*, 105.

[28] Prescot, B.; Steinmetz, W.; Thomas, G. J. Jr. *Biopolymers* **1984**, *23*, 235.

[29] DiRico, D. E., Jr.; Keller, P. B.; Hartman, K. A. *Nucl. Acids Res.* **1985**, *13*, 251.

[30] Keller, P. B.; Hartman, K. A. *Spectrochim. Acta.* **1986**, *42A*, 299.

[31] Spiro, T. G.; Biological applications of Raman spectroscopy. John Wiley & Sons, New York, 1987.

[32] Langlais, M.; Tajmir-Riahi, H. A.; Savoie, R. *Biopolymers* **1990**, *30*, 743.

[33] Starikov, E. B.; Semenov, M.A.; Maleev, V. Y.; Gasan. I. A. *Biopolymers* **1991**, *31,* 255.

[34] Kanakis, C.D.; Nafisi, Sh.; Rajabi, M.; Shadaloi, A.; Tarantilis, P. A.; Polissiou, M. G.; Bariyanga, J.; Tajmir-Riahi, H. A. *Spectroscopy* **2009**, *23*, 29.

[35] Tajmir-Riahi, H. A.; C.N'soukpoé-Kossi, C. N.; Joly, D. *Spectroscopy* **2009**, *23*, 81.

[36] Marty, R.; N'Soukpoe-Kossi, C. N.; Charbonneau, D.; Weinert, C. M.; Kreplak, L.; Tajmir-Riahi, H. A. *Nucl. Acids Res.* **2009**, *37*, 849.

[37] Polyanichko, A. M.; Andrushchenko, V. V.; Chikhirzhina, E. V.; Vorob'ev, V. I.; Wieser, H. *Nucl. Acids Res.* **2004**, *32*, 989.

[38] Andrushchenko, V.; Wieser, H.; Bour, P. *J. Phys. Chem. B* **2002**, *106*, 12623.

[39] Ahmed Ouameur, A.; Malonga, H.; Neault, J.F.; Diamantoglou, S.; Tajmir-Riahi, H.A. *Can. J. Chem.* **2004**, *82*, 1112.

[40] Ahmed Ouameur, A.; Marty, R.; Neault, J. F. *DNA Cell Biol.* **2004**, *23*, 783.

[41] Nafisi, S.; Malekabady, Z. M.; Khalilzadeh, M. A. *DNA Cell Boil.* **2010**, *29*, 753.